SLAC-PUB-797

# VACUUM SYSTEM FOR STANFORD STORAGE RING, SPEAR*

U. Cummings, N. Dean, F. Johnson, J. Jurow, J. Voss

## ERRATA

1. On page 4, the electron bombardment dose should be $3.6 \times 10^{6}$ instead of $3.6 \times 10^{3}$.

2. On page 5, the total power should be 54 KW instead of 5.4.

3. On page 6, at the top of the page, it should read, "between each of the 17 modules" instead of "between each of the 17 bending magnets".

4. On page 9, at the top of the page, it should read, "no detectable leaks" instead of "no dectable leads".

5. On page 9, in the middle of the page it should read, "half-hard" instead of "dead soft" copper gaskets.

*Work supported by the U. S. Atomic Energy Commission under Contract No. AT(04-3)-515.

SLAC-PUB-797
September 1970
(EXP) & (EXPI)

# VACUUM SYSTEM FOR STANFORD STORAGE RING, SPEAR*

U. Cummings, N. Dean, F. Johnson, J. Jurow, J. Voss

Stanford Linear Accelerator Center
Stanford University, Stanford, California 94305

## ABSTRACT

Due to its unusual geometry and gas load, the SPEAR vacuum system incorporates several unique design features. The system consists of an aluminum chamber in the form of a 200-foot diameter ring which must achieve a pressure in the $10^{-9}$ Torr range with a large gas load due to synchrotron radiation induced desorption. Since the system is conductance limited, it was necessary to develop distributed sputter ion pumps located within the chamber proper. A large number of aluminum-to-stainless steel interfaces required the development and testing of various flange arrangements which would withstand a bakeout to $200^{\circ}$C.

(To be presented at the 17th National Vacuum Symposium, Washington, D.C., October 20-23, 1970)

*Work support by the U. S. Atomic Energy Commission under Contract No. AT(04-5)-515.

# I. INTRODUCTION

The Stanford Positron-Electron Asymmetric Ring (SPEAR)[1] is a high energy physics facility proposed for construction at the Stanford Linear Accelerator Center (SLAC). Beams of electrons and positrons of 0.5 ampere each and an energy of up to 2 GeV will be injected into counter-rotating orbits in a single vacuum chamber. The beams are constrained to their circular orbits by 17 pairs of bending magnets and are focused and stabilized by an arrangement of quadrupole and sextupole magnets. With a vacuum of $10^{-9}$ Torr the beams can be stored for up to several hours. The actual physics experiments take place when the beams are made to collide in one of the two interaction regions. The interaction energy (center-of-mass energy) for a collision of this type is several orders of magnitude greater than the energy achieved with the conventional collision between a particle beam and a stationary target.

The vacuum system design criteria are determined by the requirement of maintaining an adequate beam life time which is limited, in part, by interactions between the beam particles and residual gas molecules in the vacuum chamber. In addition to the more or less conventional problems of a large vacuum system (approximately 3000 liters and an area of 130 $m^2$), the storage ring vacuum system must also handle the gas desorbed as a result of synchrotron radiation. Typically, the system pressure may rise two or three orders of magnitude when the beam is circulating in the chamber.

Most of the vacuum chamber will consist of 15.6 cm by 4.4 cm by 9.14 meters long aluminum extrusions which will be mounted on one of 17 modules consisting of two bending magnets, three quadrupoles and three sextupoles. A cross section of the extrusion is shown on Fig. 1. In the straight sections between the bending modules, the chamber will consist of standard aluminum tubing. One 80 liter/sec

ion pump will be provided at each straight section. During operation, major portions of the gas load will be pumped by distributed ion pumps located within the bending magnets. Sublimation pumps and turbo-molecular pumps will be provided for initial pump-down and bake-out.

## II. GAS DESORPTION

Experiments have shown that photons will desorb between $10^{-8}$ and $10^{-6}$ gas molecules per incident photon.[2] However, during actual operation of the Stanford-Princeton Storage Ring the gas desorption was as much as 700 times higher than what would be expected from photons alone. This higher yield has been explained as a two-step process in which photoelectrons are released by the synchrotron radiation and then returned to the wall of the vacuum chamber. Gas desorption may occur both during ejection and return of the photoelectrons. Calculations show that reasonable photoelectric coefficients and well-known electron induced desorption probabilities can explain the observed desorption rates.

Since there are no photon sources of sufficient energy and intensity for direct tests of our parameters, we have had to depend on calculations for the photoelectric coefficients and direct measurement of electron induced desorption. The electron desorption is discussed in detail below. Calculations of the photoelectric coefficients, based on work by Ganeev and Izrailev[3] indicate that the coefficients may be reduced by a factor of 3 or 4 if the photons impinge close to a normal angle with the wall. For this reason it was decided to corrugate the inner wall of the vacuum chamber which receives the syncrotron radiation. It has also been shown at SLAC that the electron desorption from aluminum is a factor of 2 or 3 lower than from stainless steel. This has been one of the prime factors in selecting aluminum as the material for the vacuum chamber.

There is a considerable literature on electron induced desorption of gases from metals and the work done at SLAC was summarized in a paper presented at the Fourth International Vacuum Congress.[4] Almost all of the previous work was concerned with developing an understanding of the mechanisms involved and were undertaken on very small systems. We felt that it would be advisable to check these results on a large system whose geometry would be similar to that of SPEAR.

The test vacuum chamber was a 3.2 m length of actual extrusion which will be used on SPEAR. The pump was a 400 liter/sec Varian Vac-ion pump with 2.2 cm diameter conductance limiting orifice at the inlet flange. The bombarding electron source was a 30 cm long tungsten filament suspended near the top of the chamber. The accelerating voltage of 400 eV was furnished by a regulated dc power supply and the bombarding current was controlled by manually varying the filament heating current. The chamber was also provided with a leak valve for introducing known gases. The total pressure was measured by two ionization gauges. Partial pressure and gas spectra were measured by a CEC-613 Residual Gas Analyzer. Fast decay rates for calculating the electron desorption rates were measured by recording the output of the residual gas analyzer on a Sanborn 7700 recorder.

The test results show that the electron desorption rates for carbon monoxide vary from an initial value of $2.5 \times 10^{-2}$ molecules per electron before bake-out to a final value of $4.5 \times 10^{-7}$ molecules per electron after bake-out and an electron bombardment dose of $3.6 \times 10^{3}$ milliamp-sec/cm$^2$. These values agree well with other published results and are lower than the value of $4.7 \times 10^{-6}$ molecules/electron which was used in our design calculations.

The acutal mechanism of electron induced desorption is far from completely understood, but we may safely say that the desorption rate is a function of:

a. The bombarding voltage.

b. The gas species involved.

c. The surface coverage which is determined by the previous gas exposure, the previous bombardment history, and the pressure in the system.

d. There is also considerable evidence that the desorption may be effected by diffusion of gas from the bulk of the metal.

In light of this, it is evident that it is not sufficient to determine only desorption rates, but it is also necessary to understand the rate at which the electron desorption decays. The typical decay curves shown on Fig. 2 agree quite well with the previous work which was done at SLAC on smaller systems.

The major gas components were carbon monoxide and hydrogen which is typical for electron bombardment. Methane which is also a result of electron bombardment in the presence of carbon and hydrogen was also present.

## III. SYSTEM PRESSURE

The syncrotron radiation impinging on the vacuum chamber wall is not uniform but is concentrated inside the bending magnets. The total power which must be absorbed by the chamber wall is 5.4 kW and the maximum power density in the plane of the beam orbit will be about 370 watts/cm$^2$. The outside wall of the vacuum chamber is provided with a cooling water channel as shown on Fig. 1. The temperature rise from the water to the inside wall of the chamber will be less than 15$^{o}$C.

The distribution of the gas load will, of course, coincide with the distribution of the synchrotron radiation which makes the system highly conductance limited.

Our calculations show that a 1000 liter/sec pump would be required between each of the 17 bending magnets in order to maintain a pressure of $5.0 \times 10^{-9}$ Torr. In order to reduce costs and for better operation we have designed a distributed sputter ion pump which is located within the bending magnets adjacent to the major portion of the gas load.

## IV. DISTRIBUTED SPUTTER-ION PUMPS

The distributed sputter-ion pump, shown on Figs. 1 and 3, consists of an array of tubular cells in which gas molecules are ionized by the action of spiraling electrons. The ions are electrostatically accelerated onto the titanium plates where sputtering ensues. The pumps are mounted inside the vacuum chamber between the pole faces of the storage ring beam-bending magnets. The field of these magnets is utilized to constrain the electrons to their spiral paths within the pump cells.

The pump anode consists of 185 tubular cells which are 1.25 cm in diameter by 2.80 cm high and are made of 0.041 cm thick, type 304 stainless steel tubing. The cells are spot-welded together to form a two cell wide linear array. The entire anode array is supported and centered by shielded insulators which are mounted on the pump cathode. The cathode consists of upper and lower titanium plates which are 0.23 cm thick by 3.55 cm wide. The titanium is 99.8% pure. A perforated aluminum screen serves as a sputter shield to protect the chamber from titanium deposits as well as a ground screen to avoid perturbation of the electron-positron beams. The entire structure is firmly fixed inside the vacuum chamber.

Test models of the pump were assembled inside a 3.5 m long aluminum vacuum chamber having a 12.5 cm by 5.1 cm cross section. The pressure was

measured by two Bayard-Alpert gauges as well as with a residual gas analyzer. Test gases were introduced with a Q-meter which metered the flow in the range from $10^{-2}$ to $10^{-6}$ Torr liter/sec.

The system was initially pumped down with an 8 liter/sec ion pump and baked to 200°C for 48 hours. The system base pressure was $1 \times 10^{-8}$ Torr. The distributed pump was then turned on with an accelerating voltage of 7.3 KeV and pumping was continued for twenty-four hours after which time the base pressure was $5 \times 10^{-10}$ Torr. Steady state, metered gas flows were introduced and the speed was calculated by:

$$S = \frac{Q}{P_2 - P_1}$$

where:

S = pumping speed in liter/sec

Q = throughput in Torr liter/sec

$P_1$ = pressure before introduction of gas, Torr

$P_2$ = pressure after introduction of gas, Torr

Measurements for nitrogen were made in the range between $3.5 \times 10^{-8}$ and $6.0 \times 10^{-6}$ Torr. Speed measurements were also made for argon, helium, hydrogen and carbon monoxide. Tests were made on pumps with 2.50 cm diameter cells as well as 1.25 cm diameter cells.

Some of the test results are given on Fig. 4 which shows the nitrogen pumping speed as a function of magnetic field strength. It will be noted that the pumping speed is essentially constant for fields stronger than 3.5 kilogauss.

The pumping speed for carbon monoxide was significantly higher than for nitrogen at all pressures. The pumping speed for pure hydrogen was about one-third of the speed for nitrogen. However, the pumping speed for a mixture of 90% hydrogen and 10% carbon monoxide was nearly two-thirds of the nitrogen speed.

The pumping speed increased as a function of the accelerating voltage up to 7.0 KeV after which it remained constant. The relationship between pumping speed and magnetic field was in accordance with that given by Jensen[5] in 1961.

The pumps showed no saturation or degradation effects after pumping 14 Torr-liters of a combined gas load consisting of 50% hydrogen and 50% carbon monoxide which corresponds to approximately two years of storage ring running time.

## V. VACUUM CHAMBER FABRICATION

Two advantages gained from the use of aluminum for the vacuum chamber material are the reduction in the electron induced gas desorption and the high thermal conductivity necessary to dissipate the intense local thermal load in the plane of the circulating beams. The other major advantage is the economy of using an extruded section rather than a welded built up section. We have conducted extensive tests to assure ourselves of the vacuum integrity of these large extrusions. The extrusions were fabricated from 12-inch diameter billets of 6061 aluminum and were extruded at a temperature between 430° C and 510°C at an extrusion speed of about 9 feet/minute. The ends were then cropped and the extrusions were heat treated at to the T-6511 condition.

The mechanical integrity of the blends (where the metal flows around the die supports) were tested by driving wedges into the ends until the metal ruptured. In most cases the rupture did not occur at the blends. The vacuum integrity was verified by repeated tests under bake-out conditions. Several samples of full length extrusions were cleaned for vacuum, pumped down, thermally cycled to 200° C and leak checked with a helium leak detector having a sensitivity of $2 \times 10^{-10}$ std cc of helium/sec. In addition, the blend

between the chamber proper and the water passage was checked by pressurizing the water chamber with helium. No detectable leads were found. During these bake-out tests the pressure varied between $10^{-7}$ and $10^{-9}$ Torr.

## V. STAINLESS STEEL - ALUMINUM FLANGES

There are a large number of flanged connections required on the ring, both between adjoining sections and between the ring and various ports for pumps, feedthroughs and instrumentation. Many of these connections will require stainless steel to aluminum flange pairs which present some difficulty because of the differential expansion which occurs during bake-out. We have tested a large number of Hall flanges using dead-soft copper gaskets which are captive in a bevel-edged groove. These flanges are self-aligning and the sealing surface is self-protected. The test results are summarized in Table 1.

An alternative stainless steel to aluminum joint which utilizes explosive bonding is also being investigated. Preliminary results obtained at the time of writing indicate that these joints will be reliable under the required conditions.

## VI. ACKNOWLEDGEMENTS

The authors would like to thank E. L. Garwin and E. W. Hoyt for many helpful discussions; R. R. Gaxiola, J. A. Pope, T. J. Sanchez and R. M. Pickup for their assistance in preparing equipment and conducting tests.

## REFERENCES


1. SPEAR Design Report, Stanford Linear Accelerator Center, Stanford, California, (1969).
2. R. O. Adams and E. E. Donaldson, J. Chem, Phys. 2, 770 (1965).
3. A. S. Ganeev and I. M. Izrailev, Sov. Phys. -Tech. Phys. 6, 270 (1961).
4. E. L. Garwin, E. W. Hoyt, M. Rabinowitz, J. Jurow, Proc. of the Fourth Inter. Vacuum Congress, (1968) (Manchester); p. 131.
5. R. L. Jepsen, J. Appl. Phys. 32, 2619-2626 (1961).

TABLE 1

ALUMINUM TO STAINLESS-STEEL FLANGE TESTS

| Flange Size (inches OD) | Number of Bolts | Number of Bake-out Cycles* | Number of Gasket Changes |
|---|---|---|---|
| 2-1/8 | 6 1/4"-28 | 572 | 34 |
| 2-3/4 | 6 1/4"-28 | 1254 | 57 |
| 4-1/2 | 8 5/16"-24 | 69 | 5 |
| 6 | 16 5/16"-24 | 148 | 5 |
| 8 | 20 5/16"-24 | 152 | 14 |

*Bake-out cycles between 20° C and 180° C.

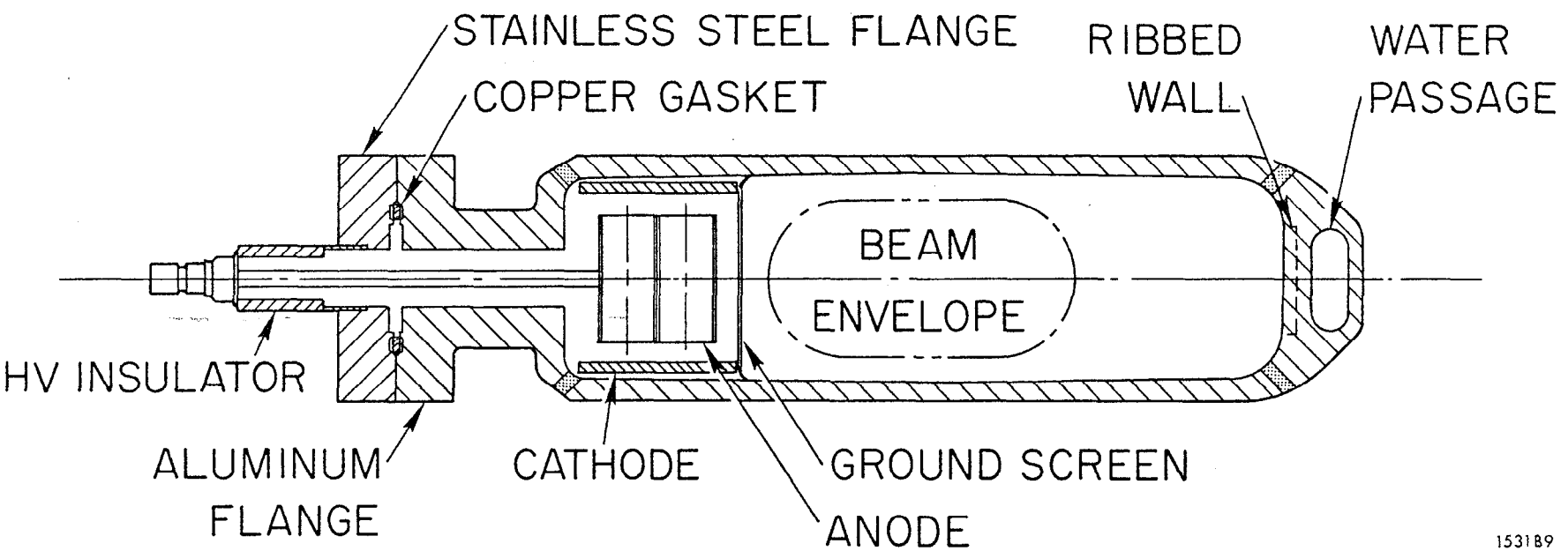


Fig. 1

SPEAR Vacuum Chamber cross section.

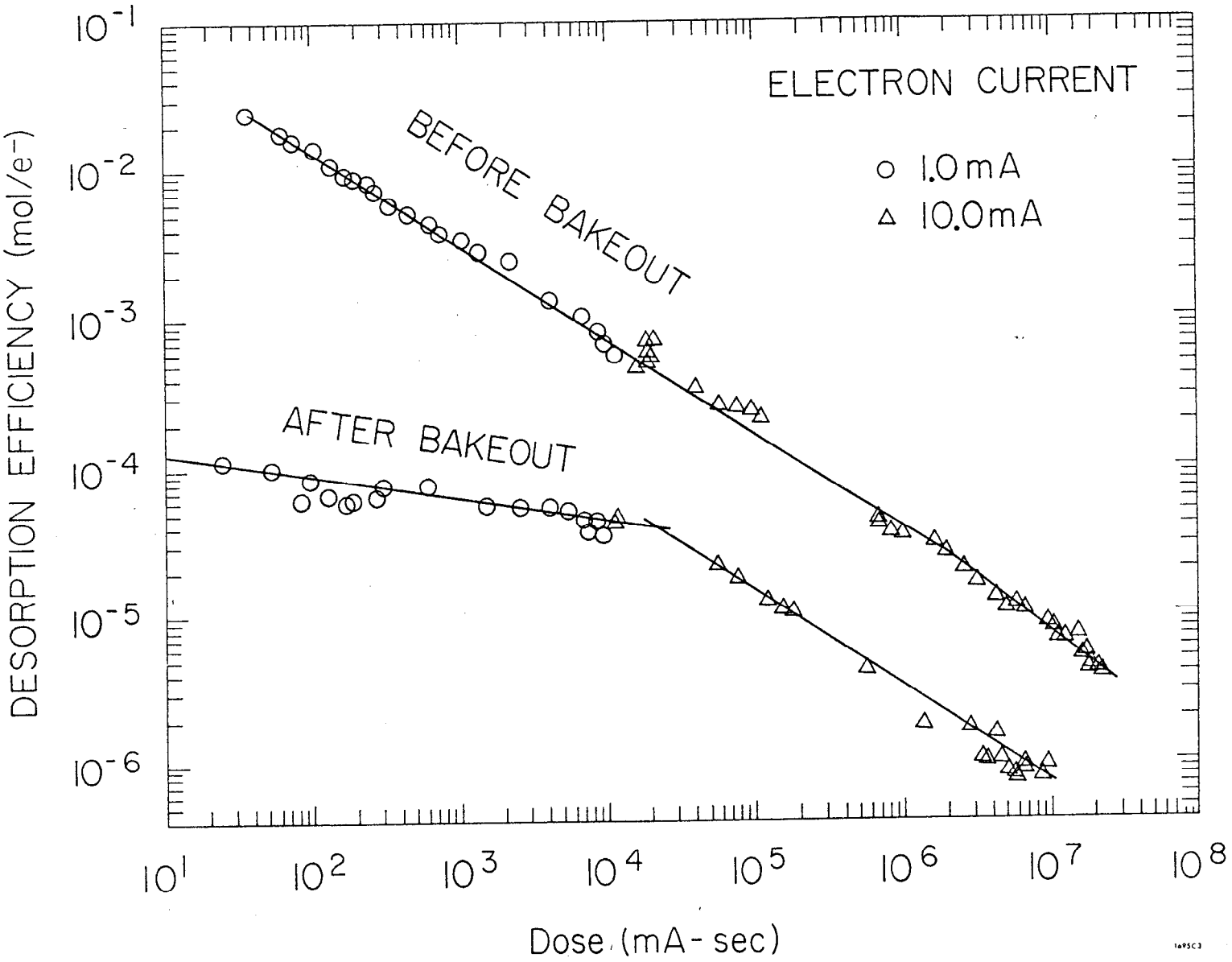


Fig. 2

Electron desorption rates.

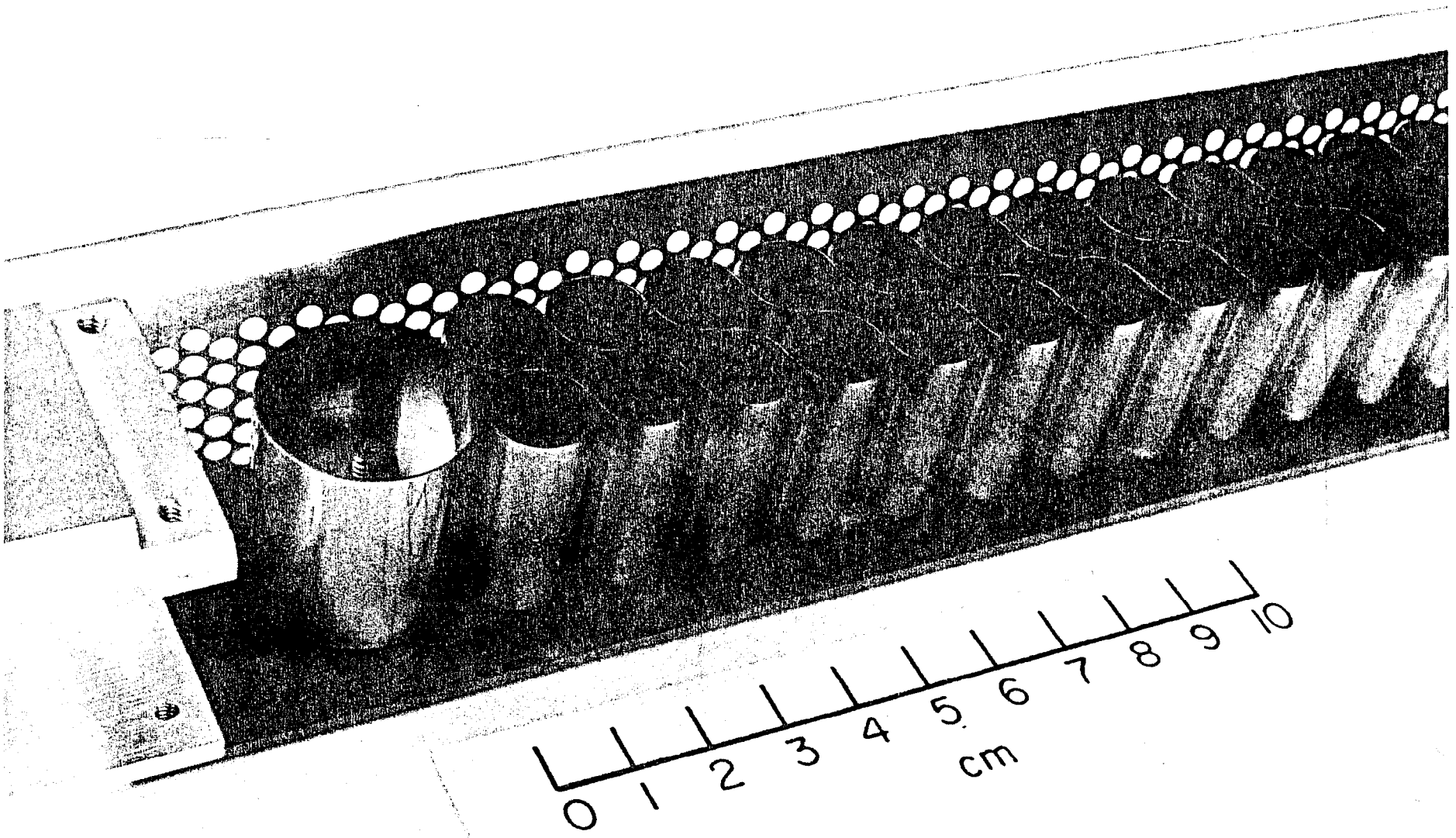


Fig. 3

1695A4

Distributed sputter-ion pump.

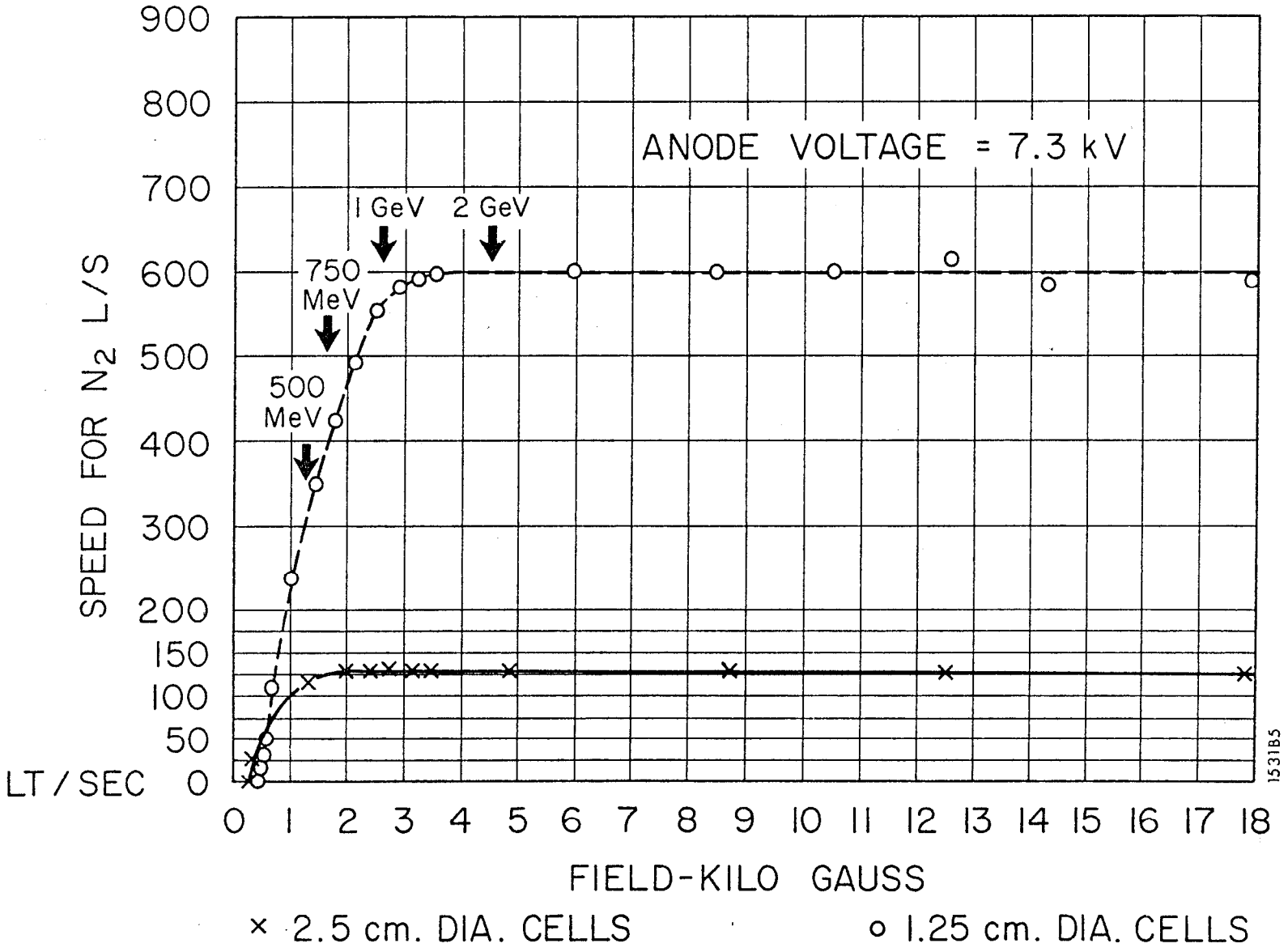


**Fig. 4**

Pump speeds.